Hindawi
International Journal of Polymer Science
Volume 2023, Article ID 2541384, 13 pages
https://doi.org/10.1155/2023/2541384

Research Article

Design and Development of Polymer-Based Optical Fiber Sensor for GAIT Analysis

Mamidipaka Hema,[1] **Jami Venkata Suman**,[2] **Boddepalli Kiran Kumar**,[3] **and Adisu Haile**[4]

[1]*Department of ECE, JNTU-GV College of Engineering, Vizianagaram, India*
[2]*Department of ECE, GMR Institute of Technology (A), Rajam, India*
[3]*Department of CSE, Aditya College of Engineering, Surampalem, India*
[4]*Department of Mechanical Engineering, WOLLO University, Kombolcha Institute of Technology, P.O. Box no: 208, Kombolcha, Ethiopia*

Correspondence should be addressed to Adisu Haile; adisu.haile@wu.edu.et

Received 21 July 2022; Revised 29 October 2022; Accepted 27 January 2023; Published 20 February 2023

Academic Editor: Adam Khan M

In the present scenario like COVID-19 pandemic, to maintain physical distance, the gait-based biometric is a must. Human gait identification is a very difficult process, but it is a suitable distance biometric that also gives good results at low resolution conditions even with face features that are not clear. This study describes the construction of a smart carpet that measures ground response force (GRF) and spatio-temporal gait parameters (STGP) using a polymer optical fiber sensor (POFS). The suggested carpet contains two light detection units for acquiring signals. Each unit obtains response from 10 nearby sensors. There are 20 intensity deviation sensors on a fiber. Light-emitting diodes (LED) are triggered successively, using the multiplexing approach that is being employed. Multiplexing is dependent on coupling among the LED and POFS sections. Results of walking experiments performed on the smart carpet suggested that certain parameters, including step length, stride length, cadence, and stance time, might be used to estimate the GRF and STGP. The results enable the detection of gait, including the swing phase, stance, stance length, and double supporting periods. The suggested carpet is dependable, reasonably priced equipment for gait acquisition in a variety of applications. Using the sensor data, gait recognition is performed using genetic algorithm (GA) and particle swarm optimization (PSO) technique. GA- and PSO-based gait template analyses are performed to extract the features with respect to the gait signals obtained from polymer optical gait sensors (POGS). The techniques used for classification of the obtained signals are random forest (RF) and support vector machine (SVM). The accuracy, sensitivity, and specificity results are obtained using SVM classifier and RF classifier. The results obtained using both classifiers are compared.

1. Introduction

Utilizing biometric information, identity recognition is being done in many scenarios. Even gender recognition and age estimation are being done by such information. Human age estimation has emerged as an important area of research [1], such that minors can be prevented from purchase of banned items and also access of inappropriate web pages. Further, elderly monitoring and human–computer interaction are feasible. Initially, age estimation was done on facial features. At distance, the facial features have low resolution on constrained details [2]. Every gait cycle consists of two steps and spans the time between the first time an event occurs with a particular foot and the next time it occurs with the same foot. Due to their superior elasticity, reduced Young's modulus, better strain limitations, impact strength, and shock resistance, polymer optical fibers (POFs) outperform silica optical fibers [3]. The use of POF for gait

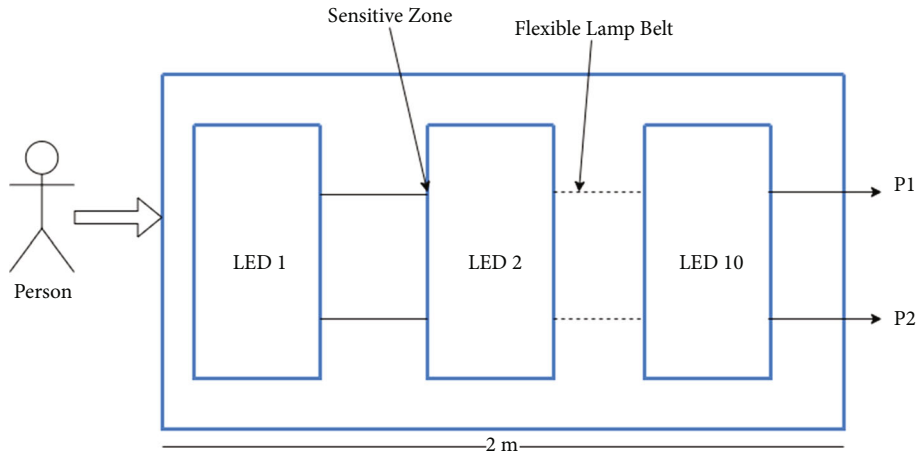

Figure 1: Structure of FOPS smart carpet for gait analysis.

examination has several applications in the clinical setting, including sensors for tracking joints angular movement, heel pressure, gait frequency, and foot positioning during the stride. Over the years, many POF sensor designs have been put forth, fiber Bragg gratings (FBGs), and interferometers. In terms of cost, manufacturing complexity, and signal processing simplicity, intensity variation-based sensors outperform the others. Since each sensor would need a photo-detector and a light generator, the absence of multiplexing abilities poses a significant obstacle to the implementation of intensity deviation sensors in the measurement of multiple parameters.

In Leal-Junior et al. [4], an insole POF-based gait signal detector and an intensity deviation POF curve sensor were created. For the practical testing of the sensors, a robotic leg and an electrical stimulating system for gait intervention were utilized. A method to monitor ground reaction force (GRF) throughout the gait phase was described in Leal-Junior et al. [5]. Because of the viscous elasticity, this polymer is not able to respond in accordance with stress consistently. Therefore, a method compensating for this impact is also suggested. Avellar et al. [6] created an intelligent carpet for measuring gait patterns and GRF built on POF. One fiber of the recommended carpet includes amplitude variability sensors and two photodiodes for acquiring signal. Multiplexing technology is centred on coupling among the luminaires and POF longitudinal portions. Specifically, built wearable foot sensors implanted in the shoe liner were used by Bucinskas et al. [7] to develop a system for fall prediction. By analysing, parameters such as weight, step size, and timing of phase enable gait evaluation.

A multiplexing strategy relying on light source coupling was presented in as a solution to this problem. In this technology, photo-detectors are placed above POF edges; measure the power of sensors' optical fluctuation during the activation of light sources. This approach yields better spatial resolution. Additionally, compared to other systems, the intensity deviation multiplexing approach produces a device at a cheaper cost [8]. Involving a mainframe can improve surveillance systems' intelligence, analyse customs, and allow robots [9]. Artificial intelligence-based gender categorization may utilize facial [10], vocal [11], or gait [12] inputs. Among these, gait has become the most sophisticated feature, being detected from a distance [13]. Many pioneering works on this have been reported. Furthermore, gait can be utilized for gender classification as done by Kozlowski and Cutting [14].

This research introduces the development of a smart platform that measures GRF and spatio-temporal gait parameters (STGP) using a polymer optical fiber sensor (POFS). The POF is made up of polymethyl methacrylate (PMMA), fluorinated polymer cladding, and polyethylene coating. The features obtained from the proposed POFS in the form of signals are given to the classifier to analyse the gait. The accuracy, sensitivity, and specificity results are computed by utilizing various classifiers such as support vector machine (SVM) and random forest (RF).

2. Materials and Methods

2.1. Polymer Optical Fiber Sensor. The construction of the POFS smart carpet is performed on a single POF arranged perpendicular to the walking direction between two 60 cm × 2 m polyethylene layers, as shown in Figure 1. The POF was composed of PMMA having 980 μm core diameter, fluorinated polymer cladding (20 μm), and polyethylene covering, which provides 2.2 mm overall diameter. A flexible light-emitting diode (LED) lamp strip that is laterally placed serves as the light source and the sensors' reactions. The FRMD-KL25Z microcontroller handles signal capture and LED control. When contrasted to industrial devices often utilized for gait assessment, this leads to a cheaper cost solution. It must also be mentioned that the planned POFS smart carpet does have a modular design, which means that the system may be built with varying numbers of LED elastic light belts across the span total span.

To ensure the appropriate length and thickness of the POF sensor, it is mounted on a permanent support. 20 sections are created laterally on the fiber with 20 cm separation. Each lateral part is outfitted with LED flexible light belts. When pressure is imparted to each lateral part, an optical power change occurs, which P1 and P2 detect. The optical power fluctuation of all 20 sensors was measured using two photo-detectors. Thus, P1 acquires the responses of 10 sensors (R_{P1}), whereas P2 acquires

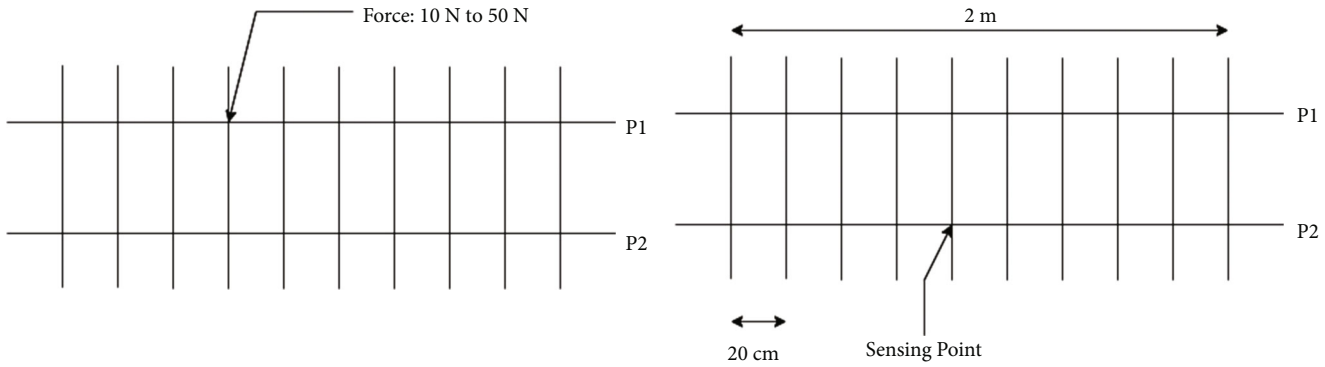

Figure 2: Characterization setup: (a) characterization of force; (b) characterization of space.

the responses of the other 10 sensors (R_{P2}). A microprocessor regulates the activation rate and sequence of one LED belt at a time. This is accomplished by activating two sensors (left and right) at the same time. The acquisition pattern is obtained from LEDs 1–10 with 30 Hz activation rate. Furthermore, the microcontroller is in charge of acquiring the optical signal detected by individual photo-detectors. Figure 2(a) depicts the setup for the characterization of force. The next approach is the characterization of space that depends on the placement of foot in specified distance markers. The purpose of this procedure is to link optical intensity with carpet distance. This assessment is connected to the force description since the sensor reaction with predetermined weights must be obtained precisely on the top of sensors. The setup for the characterization of space is depicted in Figure 2(b).

Equation (1) is used to compute the association between the attenuation of optical energy and the person's distance towards the POFS. F_0 indicates the force deployed over the POFS. F_n is the applied force alongside the fiber. n denotes the separation between F_1 and F_0. l denotes the spacing between LEDs.

$$n = \frac{F_n \cdot l}{F_0}. \tag{1}$$

Figure 3 depicts the reaction of detectors towards the loads given POFSs in the force evaluation, including the coefficient of determination (R2) and relative errors. Markers stand for the observed response, and consistent lines indicate the fitness of POFS. Figures 3(c) and 3(d) show the behaviour of load administration and a saturating propensity for larger loads. Figures 3(a) and 3(b) depict the responses of POFS. Since linearity and sensitivity are connected to the manufacture of each sensor, sensitivity varies for each light detector. Interestingly, the sensors 1 obtained by each optical detector exhibit polynomial behaviour.

2.2. Feature Extraction. There are two categories of human gait representation [15, 16]. The frequency model-based feature is not reliable. Therefore, another set of features such as force and space-based features have been used [17]. All data for experimental purpose are obtained from the POFS-based carpet. Human gait signals may be extracted using filtering and thresholding. In Wang et al. [18], extracting human gait features from signal sequences has been done. As the features of the gaits are not unique, normalization has to be done to bring to the same value.

2.2.1. Gait Energy Signals. Gait energy signal (GES) gives the spatiotemporal data of silhouette out of the whole cycle of gait. By obtaining mean of the signals yields a signal representing energy. $D(x, y)$ representing GES can be calculated by using Equation (2). Here, N gives a count of gait cycle signals. x and y indicate the gait signal coordinates.

$$D(x, y) = \frac{1}{N}\sum_{t=1}^{N} Bt(x, y). \tag{2}$$

Taking gait as the relevant characteristics [19], the gait model (GM) presents the sensitive ageing-related parameters, such as applied force and length of stride varies with age. Length of stride and force [20–22] are useful parameters for getting a useful gait-based age descriptor.

2.2.2. Dynamic Gait Energy Signal. Due to the slight movements of legs and the pressure applied on the sensor, static data from these get into GES. For reducing the impact of this static information, the dynamic information is attained with force, leg joint change and stride length represented by Equation (3).

$$I_{\mathrm{GES}}(x, y) = \begin{cases} 0 & \text{if } I_{\mathrm{GES}}(x, y) > 220 \\ 1 & \text{if } I_{\mathrm{GES}}(x, y) \neq 0 \end{cases}. \tag{3}$$

Second step computes dynamic part of GES with "AND" operator in individual signals of gait cycle sequences after acquisition of the dynamic section of the signal as indicated in Equation (4).

$$F'(x, y) = F(x, y) \times I_{\mathrm{GES}}(x, y). \tag{4}$$

2.2.3. Gait Energy Projection Model. Gait energy projection model (GPM) gives the important gender-associated

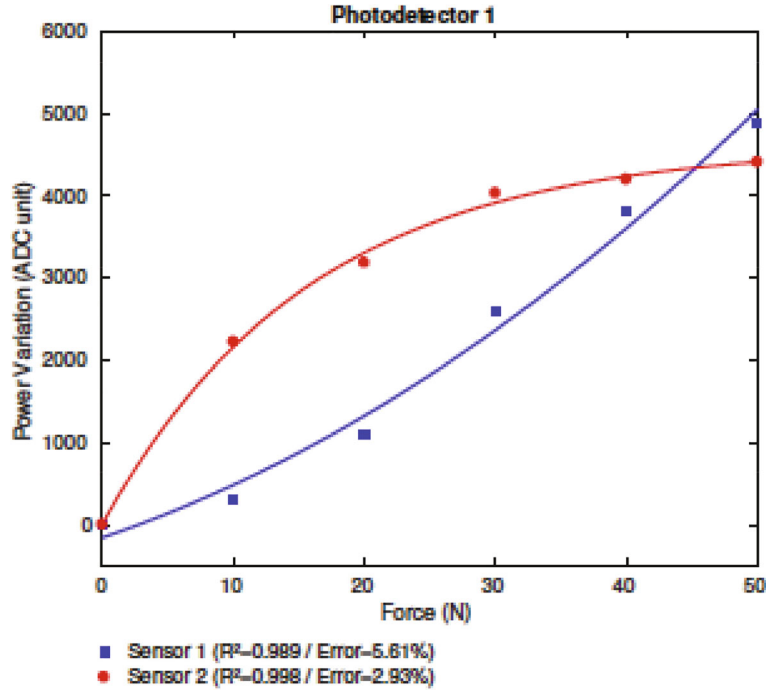

(a)

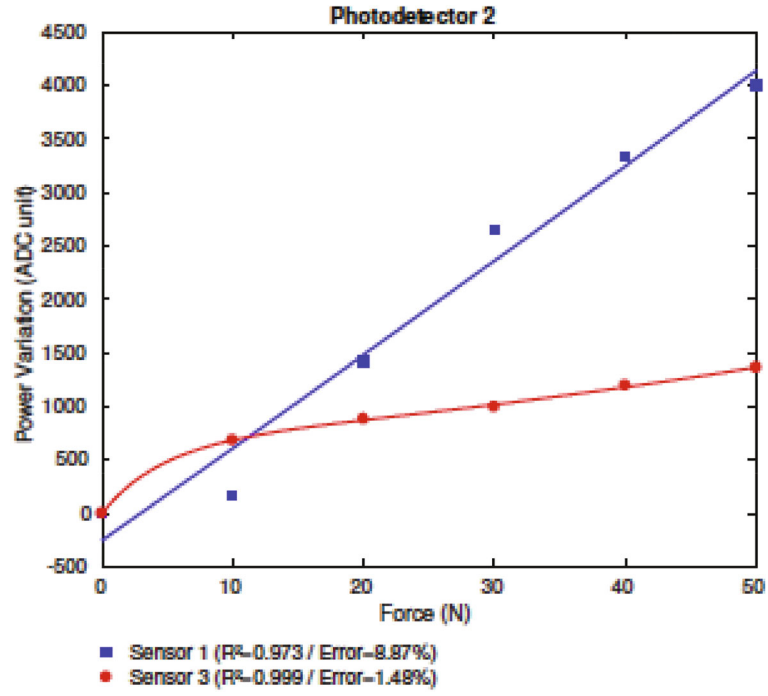

(b)

Figure 3: Continued.

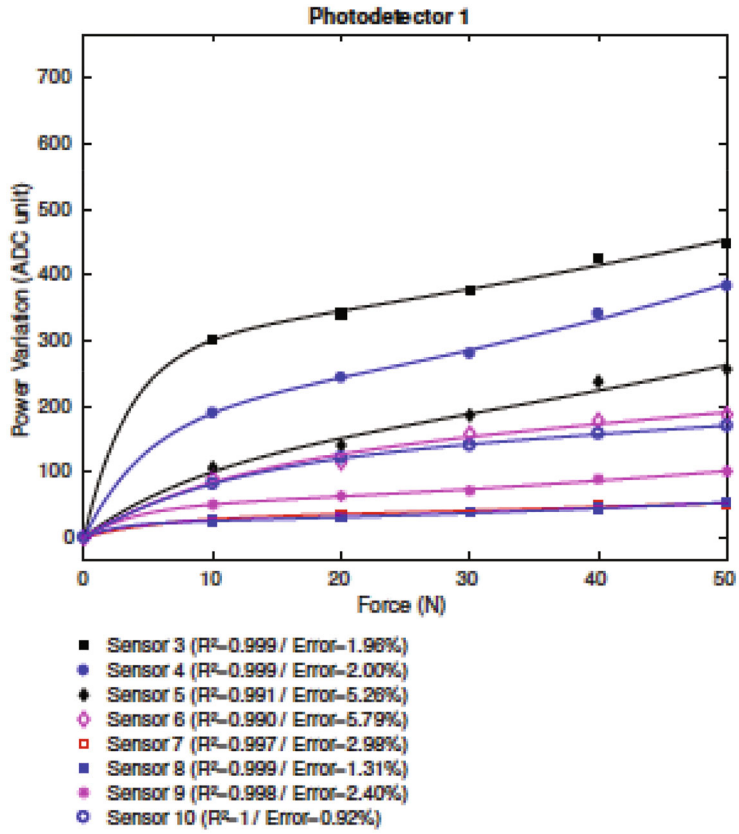

(c)

Figure 3: Continued.

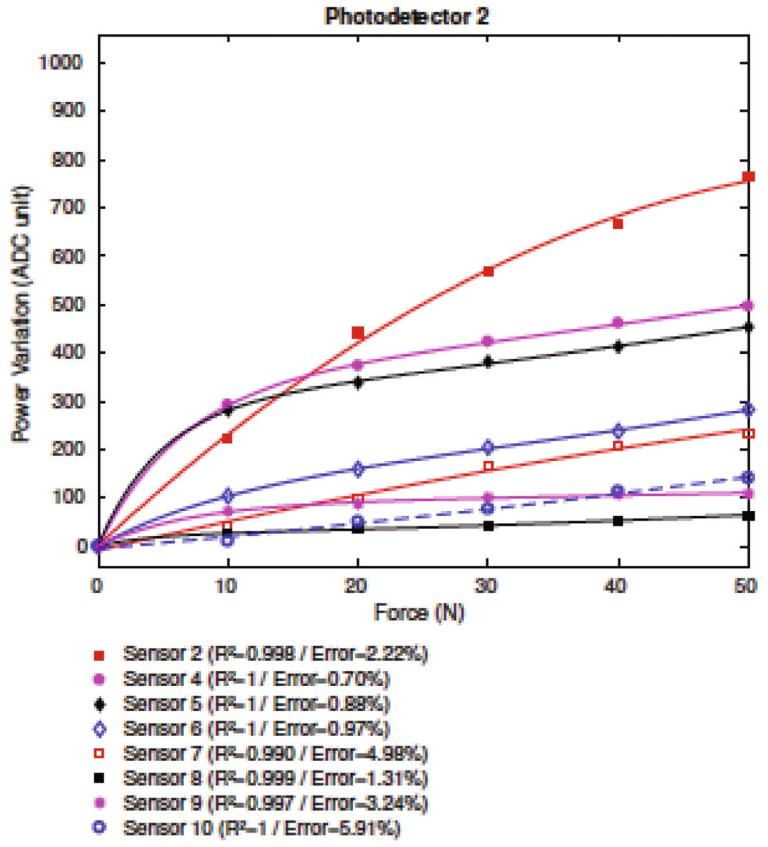

(d)

Figure 3: Force characterization response: (a) right POFS 1 and 2 with P1; (b) left POFS 1 and 3 with P2; (c) right POFS 3–10 with P1; (d) left POFS 2 and 4–10 with P2.

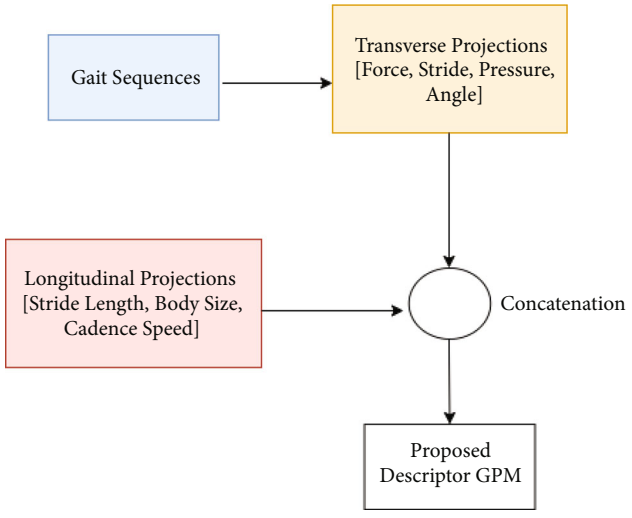

Figure 4: GPM descriptor identification.

parameter like size of body and variation in the length of stride as depicted in Figure 4.

$$\mathrm{GPM} = \left\{\mathrm{GLP}_{\mathrm{cycle}} U\, \mathrm{GTP}_{\mathrm{cycle}}\right\}. \tag{5}$$

In GPM, the two projections are gait energy longitudinal projection (GLP) and gait energy transverse projection (GTP).

$$\mathrm{GLP}_{\mathrm{cycle}} = \frac{1}{M}\sum_{i=1}^{M} GLP_i, \tag{6}$$

$$\mathrm{GTP}_{\mathrm{cycle}} = \frac{1}{M}\sum_{i=1}^{M} \mathrm{GTP}_i, \tag{7}$$

No of sets of signals = M; and i stands for the i^{th} signal vector.

2.2.4. Gradient Gait Energy Signal. Based on the averaging concept, gradient gait energy signal (GGES) has more mobile attributes than the straight forward gait signals. Kernels are required to acquire the energy of signals. Kernels create the gradient GGES pattern from energy signal of gait.

3. Feature Selection Using Genetic Algorithm

Genetic algorithm (GA) offers optimization inspired by natural solution [23, 24]. The operations are iterative and provide chromosome as a symbols string. Initial population is

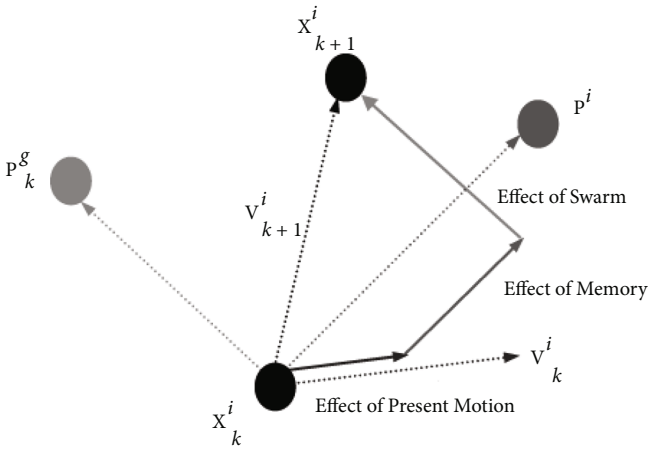

Figure 5: Velocities and positions in PSO.

an arbitrarily created set of strips. Three basic operations of genetic origin guide the search: selection, crossover, and mutation. The aim of selecting feature subset is to utilize lesser number of features, and the performance of SVM and RF may be evaluated by a validation data set for guiding the GA. Each feature subset possesses few features. By random generation, initial population is selected.

3.1. Particle Swarm Signal Template Optimization. GA and particle swarm optimization (PSO) are used to attain the borders of GES and GGES contours. The optimization process will be performed during the training and testing process. The parameters in gait signals are split into categories of weight (W_H, W_L, W_R, W_F) and stride (S_H, S_M, S_F). It is observed that the S_H and S_F are the only parameters depend on covariate conditions and S_M is independent. Swarm technique is applied in dividing the features of the signal by closely looking towards the parameters. The use of particle swarm signal template optimization (PSSTO) has more impact on the performance of the technique. So, the parameters that are retrieved can be tuned by using another overlaying optimizer. PSO includes necessary parameters such as position (X_k^i) and velocity (V_k^i) as described in Equations (8) and (9). For the i^{th} particle at k^{th} time, the minimum and maximum ranges are coined by X_{min} and X_{max}, respectively. The update in velocity at time $k + 1$ is computed using Equation (10).

$$X_k^i = X_{min} + \text{rand}\,(X_{max} - X_{min}), \tag{8}$$

$$V_k^i = \frac{X_{min} + \text{rand}\,(X_{max} - X_{min})}{\Delta t}, \tag{9}$$

$$V_{k+1}^i = wV_k^i + C_1\,\text{rand}\,\frac{(P^i - X_k^i)}{\Delta t} + C_2\,\text{rand}\,\frac{(P_k^g - X_k^i)}{\Delta t}, \tag{10}$$

where P_k^g indicates the overall best position and P^i denotes the best position. C_1 and C_2 are the coefficients. The velocity used to revise the location of particle is computed using Equation (11).

$$X_{k+1}^i = X_k^i + V_{k+1}^i \Delta t. \tag{11}$$

Updating velocity and position, and fitness computation are major operations that are repeated until convergence and are depicted in Figure 5.

4. Classification and Recognition

4.1. Training and Testing Phase. The total signals are classified into training and testing sets. In training phase, database signals are selected and applied with GES/GGES. The PSO template and GES/GGES features are contrasted with test signals. Linear discriminant analysis (LDA) is selected as classifier to recognize exact signal. Obtained signal is provided to Principal Component Analysis (PCA) for additional reduction in dimension.

4.2. Feature Reduction. For feature reduction, PCA and LDA are the optimum transform schemes. PCA discards labels of class and its target is to locate the orientation known as principal component, which maximizes the conflict. LDA computes the orientation and linear discriminants for maximization of separation. Combination of PCA and LDA is known to give good results.

4.3. SVM Classification. SVM classifier with linear kernel has been one of classifiers, which can categorize the feature vector with the help of a hyper plane [25]. The separation between the data is coined as decision hyperplane, and the separation from the hyper-plane is termed margin. Optimum target of SVM training is to obtain the hyper-plane having highest margin and to provide accurate classification [26]. Usage of linear kernel reduces the risk of over-fitting the data and increases the efficiency of classification by reducing the overall complexity.

4.4. RF Classifier. Random trees, then again, randomize the choice criteria. A random choice basis is characterized by a random characteristic and an irregular limit. Random trees, in this way, separate the preparation information on totally random characteristics [27]. This randomization primarily addresses high dimensional information and speculation. A random tree chooses an irregular element and a random edge and partitions the preparation pictures at a hub as depicted in Figure 6.

Recursively, an entire tree and thusly an accumulation of trees are assembled, which comprise a random timberland. The classification results from each tree are gathered for an info picture and regularly, a basic larger part casting a vote plot grants the subsequent class mark. In the accompanying areas, we present the utilization of RF on various related picture tasks. The features extracted consist of feature vectors from the trained data, and the trained data are given by Equation (12). Here, T_n is the elements that are present in the

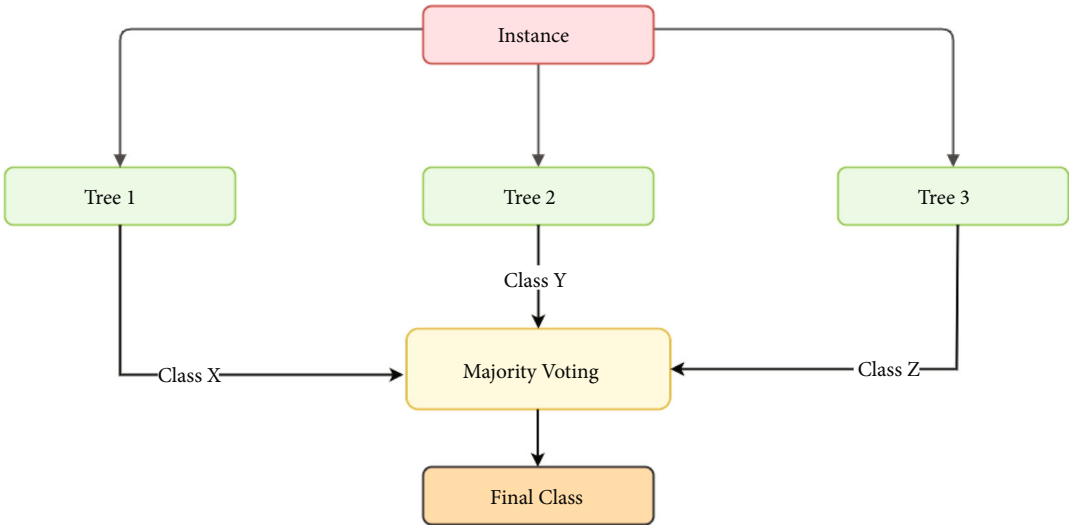

Figure 6: Random forest classifier model.

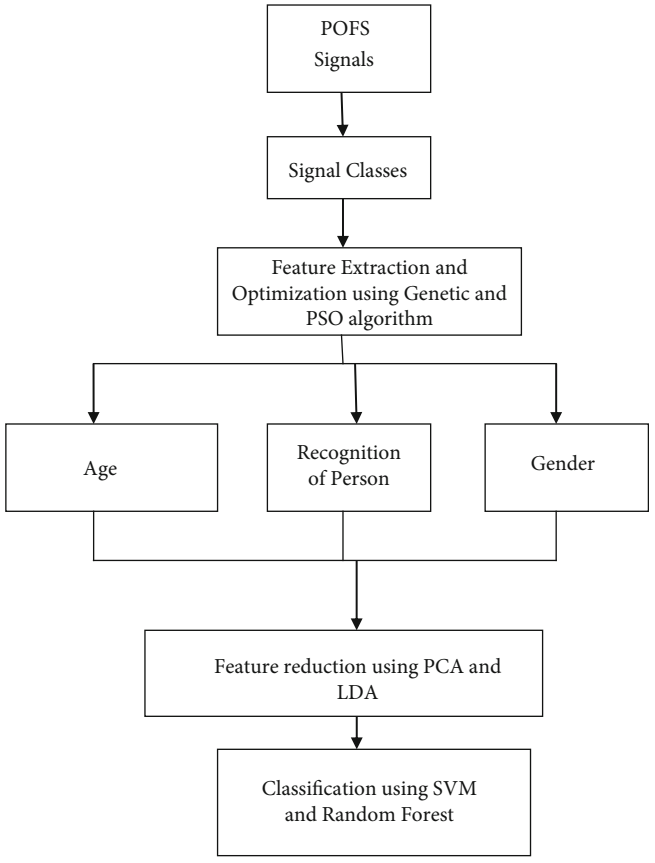

Figure 7: Design flow of proposed classification model.

data; each of the data has its own feature which is termed c_p.

$$D = T_n c_p ; n = 1, \cdots N \text{ and } p = 1, \cdots P. \quad (12)$$

The accuracy of classification increases due to the presence of decision trees, which acts the nodes to obtain the relevant data. The process flow of the proposed POFS signal-based gait classification model is provided in Figure 7.

5. Results and Discussion

The performance of SVM and RF using GA and PSO are contrasted to find out the optimum technique that

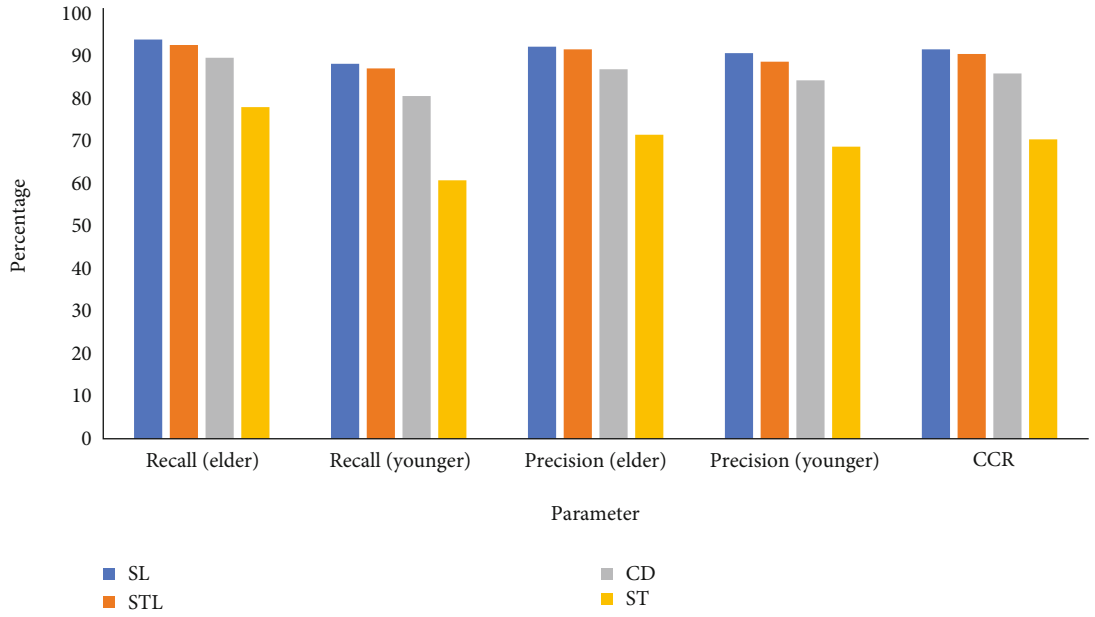

Figure 8: Age recognition with GA and SVM.

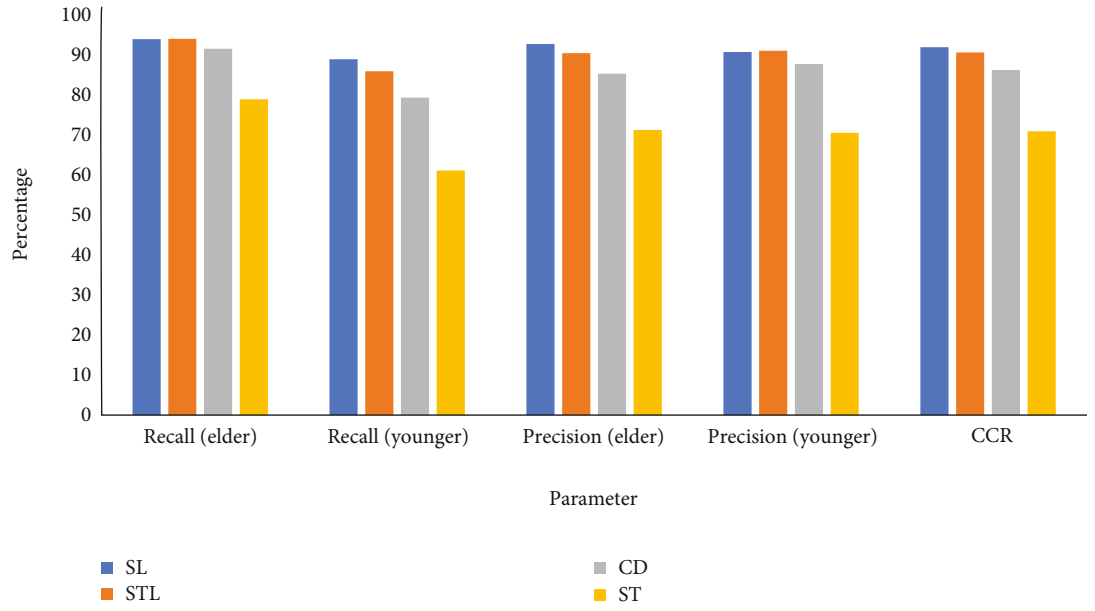

Figure 9: Age recognition with PSO and RF.

provides better results. The classifiers are provided with optimum features provided by GA and PSO algorithms. Optimal features selected are given as the input to the classifiers, and the results does not have the effect of unwanted features.

5.1. Age Recognition. Let us consider age recognition using GA and PSO optimization with various conditions. The parameters like recall, precision, and correct classification rate (CCR) are evaluated. Various descriptors such as step length (SL), stride length (STL), cadence (CD), and stance time (ST) are used for the recognition of age. For all the parameters evaluated, SL produces maximum value. So, SL can be selected as the optimum descriptor for the recognition of age. The results obtained for age recognition with GA and SVM are depicted in Figure 8.

While considering recall (elder), STL produces maximum value of 93.9%. For all the remaining parameters, descriptor SL produced maximum values. So, SL can be selected as the optimum descriptor for the recognition of age. The descriptor ST provides the lowest values for the performance parameters. The results obtained for age recognition with PSO and RF are depicted in Figure 9.

5.2. Gender Recognition. Let us consider gender recognition using GA and PSO optimization with various conditions.

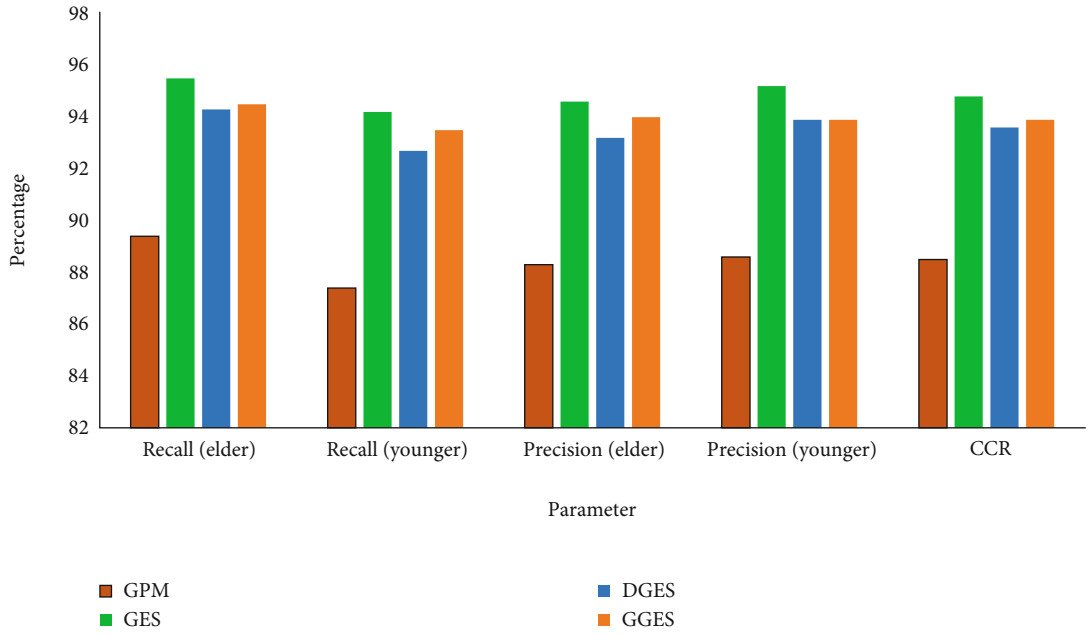

Figure 10: Gender recognition with GA and SVM.

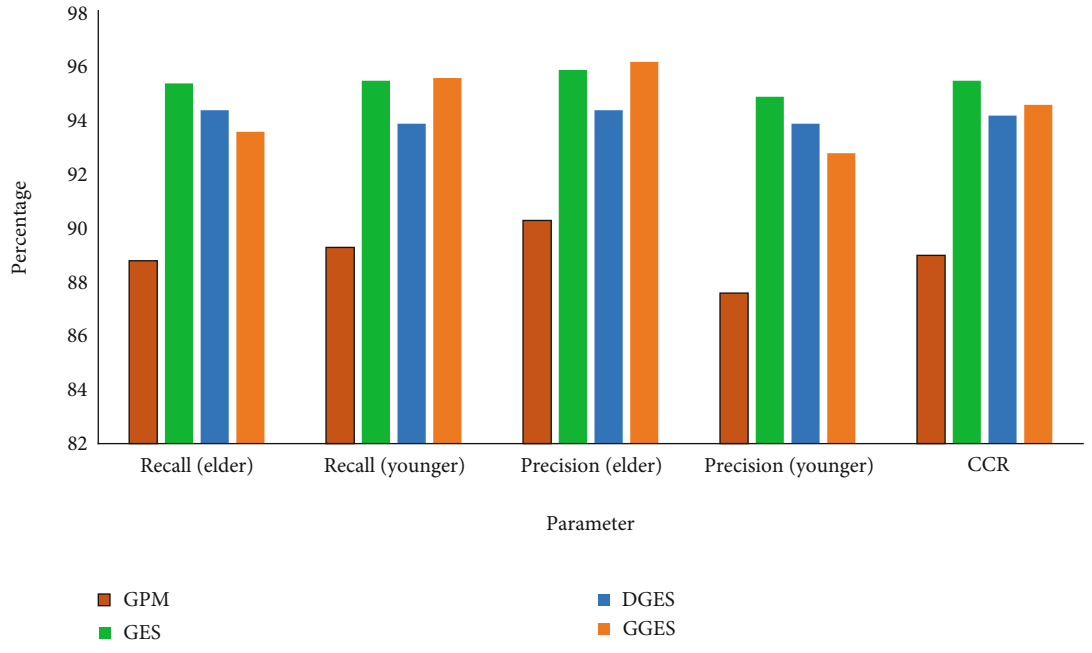

Figure 11: Gender recognition with PSO and RF.

Various descriptors such as GPM, GES, dynamic gait energy signal (DGES), and GGES are used for the recognition of gender. The parameters like recall, precision, and CCR are evaluated. During the recognition of gender using GES descriptor, maximum values are obtained for all the parameters. Lowest parameter values were obtained for the descriptor GPM. This implicates that GES is the optimum descriptor for gender recognition using GA and SVM. The results obtained are shown in Figure 10.

While performing gender recognition with PSO and RF, the usage of GGES descriptor provides maximum value 95.9% for the parameter precision (elder). Maximum values for all the remaining parameters are obtained for the descriptor GES. Lowest parameter values were obtained for the descriptor GPM. This implicates that GES is the optimum descriptor for gender recognition using PSO and RF. The results obtained are shown in Figure 11.

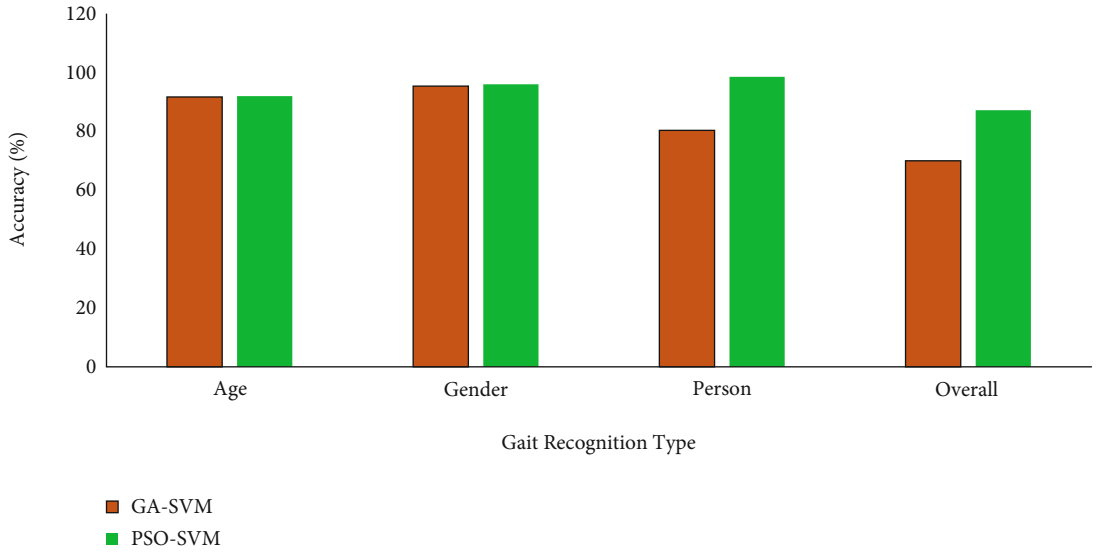

Figure 12: Accuracy using SVM classifier.

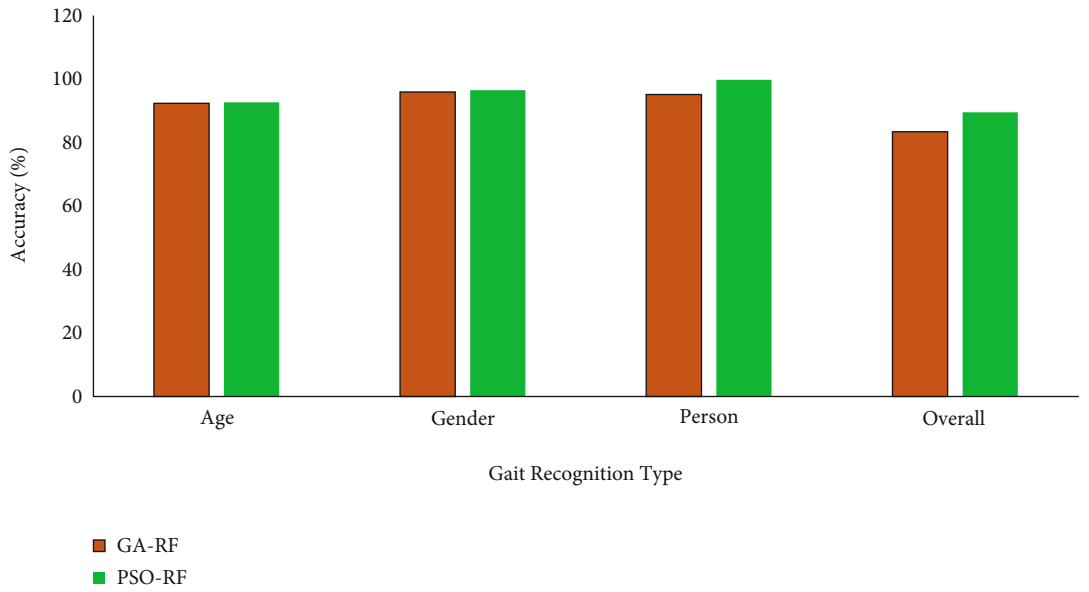

Figure 13: Accuracy using RF classifier.

5.3. Classifier Performance. SVM and RF are the two classifiers used for recognizing various gait-related human biometrics. The performance of these two classifiers is compared to find out the optimum classifier for gait classification from the signals obtained from POFS. Initially, SVM is considered with two optimization techniques such as GA and PSO. The accuracy comparison is depicted in Figure 12.

PSO-SVM provides the maximum accuracy for different gait-related analysis. So PSO is identified as the best optimizer for the selection of descriptors. The maximum overall recognition accuracy is found to be 87.16% for PSO-SVM. In the next stage of experiment, RF is considered with two optimization techniques such as GA and PSO. The accuracy comparison for RF classifier is depicted in Figure 13. In this analysis, PSO-RF provides the maximum accuracy for different gait-related analysis. So PSO is identified as the best optimizer for the selection of descriptors while using RF classifier.

From Figures 12 and 13, it is clear that the maximum value for overall accuracy of 89.58% is provided by PSO-RF classifier. This value is 2.42% more than that of PSO-SVM classifier. So, the PSO-RF classifier can categorize signals obtained from POFS in an efficient way.

6. Conclusion

This study described the construction of a smart carpet that measures GRF and STGP using a POFS. The suggested carpet contains two light detection units for acquiring signals. Each unit is capable of obtaining response from 10 nearby sensors. There are 20 intensity deviation sensors on a fiber.

One LED is triggered successively using the multiplexing approach that is being employed. Multiplexing is dependent on coupling among the LED and POFS sections. Results of walking experiments performed on the smart carpet suggested that certain parameters, including SL, STL, CD, and ST, might be used to estimate the GRF and STGP. The results enable the detection of gait instances, including the stance and swing phases, stance length, and the double supporting periods. The suggested carpet is dependable, reasonably priced equipment for gait acquisition in a variety of applications. An optimized GA-based approach for automatic feature selection has been proposed. Using PCA and LDA, irrelevant information has been reduced. SVM and RF classifier have been used to categorize signals in terms of person age and gender. This method could provide insight into gait classification problems with an overall accuracy of 89.58%. The inclusion of polymer-based sensors (POFS) provided high quality signals, and the analysis provided better results. Major merits of using POFS are the improved signal quality and fast response.

Data Availability

Data supporting this research article are available from the corresponding author or first author on reasonable request.

Conflicts of Interest

The authors declare that they have no conflicts of interest.

References

[1] N. K. Sarah, "Using artificial neural network for human age estimation based on facial images," *Proceedings of International Conference Innovations in Information Technology*, pp. 215–219, United Arab Emirates, Abu Dhabi, UAE, 2012.

[2] J. Lu and Y. -P. Tan, "Gait-based human age estimation," *IEEE International Conference on Acoustics, Speech and Signal Processing*, pp. 1718–1721, Dallas, TX, USA, 2010.

[3] K. Peters, "Polymer optical fiber sensors-a review," *Smart Materials and Structures*, vol. 10, p. 013002, 2011.

[4] A. G. Leal-Junior, A. Frizera, L. Vargas-Valencia et al., "Polymer optical fiber sensors in wearable devices: toward novel instrumentation approaches for gait assistance devices," *IEEE Sensors Journal*, vol. 18, no. 17, pp. 7085–7092, 2018.

[5] A. G. Leal-Junior, A. Frizera, L. M. Avellar, C. Marques, and M. J. Pontes, "Polymer optical fiber for in-shoe monitoring of ground reaction forces during the gait," *IEEE Sensors Journal*, vol. 18, no. 6, pp. 2362–2368, 2018.

[6] L. M. Avellar, A. G. Leal-Junior, C. A. Diaz, C. Marques, and A. Frizera, "POF smart carpet: a multiplexed polymer optical fiber-embedded smart carpet for gait analysis," *Sensors*, vol. 19, no. 15, p. 3356, 2019.

[7] V. Bucinskas, A. Dzedzickis, J. Rozene et al., "Wearable feet pressure sensor for human gait and falling diagnosis," *Sensors*, vol. 21, no. 15, p. 5240, 2021.

[8] G. A. T. Sevilla, J. P. Rojas, H. M. Fahad et al., "Flexible and transparent silicon-on-polymer based sub-20 nm non-planar 3D FinFET for brain-architecture inspired computation," *Advanced Materials*, vol. 26, no. 18, pp. 2794–2799, 2014.

[9] L. Lee and W. Grimson, "Gait analysis for recognition and classification," *Proceedings of Fifth IEEE International Conference on Automatic Face Gesture Recognition*, pp. 155–161, Washington, USA, DC, 2002.

[10] B. A. Golomb, D. T. Lawrence, and T. J. Sejnowski, "SEXNet: a neural network identifies sex from human faces," *Proceedings of the Conference Advances in Neural Information Processing Systems*, vol. 3, pp. 572–577, 1990.

[11] H. Harb and L. Chen, "Gender identification using a general audio classifier," *Proceedings of the International Conference on Multimedia and Expo*, pp. 733–736, Washington, DC, USA, 2003.

[12] X. Li, S. J. Maybank, S. Yan, D. Tao, and D. Xu, "Gait components and their application to gender recognition," *IEEE Transactions on Systems, Man and Cybernetics Part C Applications and Reviews*, vol. 38, no. 2, pp. 145–155, 2008.

[13] J. E. Boyd and J. J. Little, "Biometric gait recognition," in *Advanced Studies in Biometrics: Summer School on Biometrics*, pp. 19–42, LCNS, 2005.

[14] L. T. Kozlowski and J. E. Cutting, "Recognizing the sex of a walker from a dynamic point-light display," *Perception & Psychophysics*, vol. 21, no. 6, pp. 575–580, 1977.

[15] G. Shakhnarovich, L. Lee, and T. Darrell, "Integrated face and gait recognition from multiple views," *Proceedings of the IEEE Conference Computer Vision and Pattern Recognition*, pp. I439–I446, CVPR, Kauai, HI, USA, 2001.

[16] L. Wang, H. Ning, T. Tan, and W. Hu, "Fusion of static and dynamic body biometrics for gait recognition," *IEEE Transactions on Circuits and Systems for Video Technology*, vol. 14, no. 2, pp. 149–158, 2004.

[17] J. Han and B. Bhanu, "Individual recognition using gait energy image," *IEEE Transactions on Pattern Analysis and Machine Intelligence*, vol. 28, no. 2, pp. 316–322, 2006.

[18] L. Wang, T. Tan, H. Ning, and W. Hu, "Silhouette analysis-based gait recognition for human identification," *IEEE Transactions on Pattern Analysis and Machine Intelligence*, vol. 25, no. 12, pp. 1505–1518, 2003.

[19] C. Wang, J. Zhang, L. Wang, J. Pu, and X. Yuan, "Human identification using temporal information preserving gait template," *IEEE Transactions on Pattern Analysis and Machine Intelligence*, vol. 34, no. 11, pp. 2164–2176, 2011.

[20] N. Mansouri, M. Aouled Issa, and Y. Ben Jemaa, "Gait-based human age classifiation using a silhouette model," *IET Biometrics*, vol. 7, no. 2, pp. 116–124, 2017.

[21] Y. Liu, T. C. Robert, and Y. Tsin, "Gait sequence analysis using frieze patterns," *Proceedings of European Conference Computer Vision*, pp. 657–671, Copenhagen, Denmark, 2002.

[22] N. Cuntoor, A. Kale, and R. Chellappa, "Combining multiple evidences for gait recognition," *Proceedings International Conference Acoustics, Speech, and Signal Processing*, pp. 33–36, IEEE, Hong Kong, 2003.

[23] A. Norouzi and A. H. Zaim, "Genetic algorithm application in optimization of wireless sensor networks," *The Scientific World Journal*, vol. 2014, p. 15, 2014.

[24] A. Masuri, O. Medina, S. Hacohen, and N. Shvalb, "Gait and trajectory optimization by self-learning for quadrupedal robots with an active back joint," *Journal of Robotics*, vol. 2020, p. 7, 2020.

[25] J. Luo, J. Tang, and X. Xiao, "Abnormal gait behavior detection for elderly based on enhanced Wigner-Ville analysis and cloud

incremental SVM learning," *Journal of Sensors*, vol. 2016, p. 18, 2016.

[26] S. M. Vasanthi and T. Jayasree, "Performance evaluation of pattern recognition networks using electromyography signal and time-domain features for the classification of hand gestures," *Proceedings of the Institution of Mechanical Engineers. Part H*, vol. 234, no. 6, pp. 639–648, 2020.

[27] A. H. Lenin, S. M. Vasanthi, and T. Jayasree, "Automated recognition of hand grasps using electromyography signal based on LWT and DTCWT of wavelet energy," *International Journal of Computational Intelligence Systems*, vol. 13, no. 1, pp. 1027–1035, 2020.